

A metal protein-attenuating compound for PET neuroimaging: Synthesis and preclinical evaluation of [11C]PBT2

Hema S. Krishnan, Vadim Bernard-Gauthier, Michael Stephen Placzek, Kenneth Dahl, Vidya Narayanaswami, Elijah Livni, Zhen Chen, Jing Yang, Thomas Lee Collier, Chongzhao Ran, Jacob M. Hooker, Steven H Liang, and Neil Vasdev

Mol. Pharmaceutics, **Just Accepted Manuscript** • DOI: 10.1021/acs.molpharmaceut.7b00936 • Publication Date (Web): 03 Jan 2018

Downloaded from <http://pubs.acs.org> on January 5, 2018

Just Accepted

“Just Accepted” manuscripts have been peer-reviewed and accepted for publication. They are posted online prior to technical editing, formatting for publication and author proofing. The American Chemical Society provides “Just Accepted” as a free service to the research community to expedite the dissemination of scientific material as soon as possible after acceptance. “Just Accepted” manuscripts appear in full in PDF format accompanied by an HTML abstract. “Just Accepted” manuscripts have been fully peer reviewed, but should not be considered the official version of record. They are accessible to all readers and citable by the Digital Object Identifier (DOI®). “Just Accepted” is an optional service offered to authors. Therefore, the “Just Accepted” Web site may not include all articles that will be published in the journal. After a manuscript is technically edited and formatted, it will be removed from the “Just Accepted” Web site and published as an ASAP article. Note that technical editing may introduce minor changes to the manuscript text and/or graphics which could affect content, and all legal disclaimers and ethical guidelines that apply to the journal pertain. ACS cannot be held responsible for errors or consequences arising from the use of information contained in these “Just Accepted” manuscripts.



1
2
3
4
5
6
7
8
9
10
11
12
13
14
15
16
17
18
19
20
21
22
23
24
25
26
27
28
29
30
31
32
33
34
35
36
37
38
39
40
41
42
43

A metal protein-attenuating compound for PET neuroimaging: Synthesis and preclinical evaluation of [¹¹C]PBT2

44
45
46
47
48
49
50
51
52
53
54
55
56
57
58
59
60

Hema S. Krishnan,^{1,2} Vadim Bernard-Gauthier,^{1,2} Michael S. Placzek,^{2,3} Kenneth Dahl,^{1,2} Vidya Narayanaswami,¹ Elijah Livni,^{1,2} Zhen Chen,¹ Jing Yang,^{2,3} Thomas L. Collier,^{1,2,4} Chongzhao Ran,^{2,3} Jacob M. Hooker^{2,3} Steven H. Liang,^{1,2,} and Neil Vasdev,^{1,2,*}*

1. Division of Nuclear Medicine and Molecular Imaging, Massachusetts General Hospital, Boston, Massachusetts 02114, United States.
2. Department of Radiology, Harvard Medical School, Boston, Massachusetts 02115, United States.
3. Athinoula A. Martinos Center for Biomedical Imaging, Massachusetts General Hospital, Charlestown, Massachusetts 02129, United States.
4. Advion Inc., Research and Development, Ithaca, New York 14850, United States.

KEYWORDS.

PBT2, ¹¹C-labeled PBT2, Metal Hypothesis of Alzheimer's Disease, Carbon-11, Positron Emission Tomography, PET, Neuroimaging, Amyloid-β plaques.

1
2
3 ABSTRACT
4
5

6
7 Dyshomeostasis or abnormal accumulation of metal ions such as copper, zinc and iron have been
8
9 linked to the pathogenesis of multiple neurodegenerative disorders including Alzheimer's disease
10
11 (AD) and Huntington's disease (HD). 5,7-Dichloro-2-((dimethylamino)methyl)quinolin-8-ol,
12
13 PBT2, is a second generation metal protein-attenuating compound that has recently advanced in
14
15 Phase II clinical trials for the treatment of AD and HD based on promising preclinical efficacy
16
17 data. Herein, we report the first radiosynthesis and preclinical positron emission tomography
18
19 (PET) neuroimaging evaluation of [¹¹C]PBT2 in rodents and nonhuman primates. Carbon-11
20
21 labeled PBT2 was synthesized in 4.8 ± 0.5% (non-decay corrected) radiochemical yield (RCY)
22
23 at end-of-synthesis, based upon [¹¹C]CH₃I (*n* = 6), with >99% radiochemical purity and 80-90
24
25 GBq/μmol molar activity (*A_m*) from the corresponding normethyl precursor. In the non-human
26
27 primate brain, [¹¹C]PBT2 uptake was extensive with peak concentration SUV_{peak} of 3.2-5.2
28
29 within 2.5-4.5 min post-injection in all cortical and sub-cortical gray matter regions (putamen >
30
31 caudate > cortex >>> white matter) followed by rapid washout from normal brain tissues.
32
33 Furthermore, it is shown that [¹¹C]PBT2 binds specifically in AD human brain tissue *in vitro*.
34
35 The results presented here, combined with the clinical data available for PBT2, warrant the
36
37 evaluation of [¹¹C]PBT2 as an exploratory PET radiotracer in humans.
38
39
40
41
42
43
44
45
46
47
48
49
50
51
52
53
54
55
56
57
58
59
60

INTRODUCTION

Alzheimer's disease (AD) is a chronic, progressive neurological disease with a high socioeconomic burden.¹ All current approved treatments only work on mitigating and managing disease symptoms and none of them address the underlying causes.² The defining neuropathologic lesions of AD are amyloid- β (A β) senile plaques and tau neurofibrillary tangles, both of which appear many years before the onset of symptoms of cognitive impairment. Traditionally, the 'Amyloid Hypothesis' postulates that A β is the proximal causative agent, and its accumulation is accompanied by oxidative stress, neuroinflammation and neurodegeneration.³⁻⁵ In addition, it has been shown that elevated levels of iron along with aggregation of copper and zinc in cerebral A β is a key characteristic in AD brains.⁶⁻⁷ This led to the formulation of the 'Metal Hypothesis of AD' which posits that the neuropathological effects of A β are bolstered by metal-A β interactions leading to the formation of stable insoluble oligomers and the production of reactive oxygen species.⁸⁻⁹ Furthermore, abnormal protein-copper interactions have been described in Huntington's (HD), Parkinson's (PD) and amyotrophic lateral sclerosis (ALS; Lou Gehrig's) diseases.¹⁰⁻¹³ This has impelled the development of several metal protein-attenuating compounds (MPACs) as potential therapeutic agents to restore metal homeostasis. The most promising leads from this compound class have been derivatives of 8-hydroxyquinoline, **1 (Figure 1)**.¹⁴⁻¹⁵ Studies in transgenic mice showed up to 49% reduction in brain A β aggregation upon treatment with 5-chloro-7-iodoquinolin-8-ol (clioquinol, CQ, **2**).¹⁶ A preliminary clinical positron emission tomography (PET) study with [¹⁸F]FDG showed improved glucose metabolism in subjects with familial AD and a promising Phase II/III clinical study in AD patients treated with CQ, but the study was terminated due to toxic by-products in the drug manufacturing process.¹⁷⁻¹⁸ The results from these studies

1 supported the development of radioiodinated [^{123}I]CQ ([^{123}I]2) for imaging patients with AD.¹⁹
2
3 However, the use of this radiotracer was hampered by radiodeiodination and low brain uptake *in*
4
5 *vivo* in both mice and humans.¹⁹⁻²⁰ Following this study, our group reported the development of
6
7 the fluorinated 8-hydroxyquinoline derivative CABS13 (**3**, **Figure 1**).²¹⁻²² In preliminary rodent
8
9 studies with transgenic and age-matched wild-type control mice, [^{18}F]CABS13 demonstrated
10
11 overall higher but transient brain uptake in the transgenic mice (~4.5 standardized uptake value,
12
13 SUV) compared to the control mice (~3 SUV). However, the tracer showed negligible brain
14
15 uptake and fast metabolism in non-human primate imaging studies.²³
16
17
18
19
20
21

22
23 *Insert Figure 1*
24
25

26 Bifunctional small molecules based on substituted anilines (L2-a, **4** and L2-b, **5**, **Figure 1**) have
27
28 also been reported.²⁴ In a separate study, the synthesis and preclinical evaluation of the carbon-
29
30 11 and fluorine-18 derivatives of L2-b was conducted and showed reasonable brain uptake in
31
32 non-human primates (~2 SUV) followed by moderate washout, yet those radiotracers have not
33
34 been advanced in further studies thus far.²⁵ PBT2 (5,7-dichloro-2-
35
36 ((dimethylamino)methyl)quinolin-8-ol, **7**, **Figure 1**) is a MPAC that was developed for the
37
38 treatment of AD which has recently been repurposed for HD.²⁶⁻³⁰ This compound is a second-
39
40 generation 8-hydroxyquinoline analog that was developed as a potential successor to CQ.
41
42 Following promising results in transgenic AD mice models wherein rapid decrease in soluble A β
43
44 and improved cognitive functions was observed *in vivo*, Prana Biotechnology began a Phase IIa
45
46 trial in Europe (EURO) with PBT2 in a small population of patients with AD.³¹ The double-
47
48 blind, randomized, placebo-controlled study found that 250 mg of PBT2 when administered over
49
50 the course of 12 weeks resulted in improved cognitive function and reduced amounts of soluble
51
52 A β in cerebrospinal fluid.³²⁻³⁴ In the second stage of this Phase II study in Australia
53
54
55
56
57
58
59
60

1
2
3 (IMAGINE/extension), patients with AD ($n = 78$) were subject to a double-blind, randomized
4 trial with 250 mg PBT2 and a placebo. The primary outcome was monitored by measurement of
5 amyloid deposition with PET scans using the gold standard amyloid imaging tracer, [^{11}C]PiB.³⁵
6
7 The results of the study did not meet the criteria set forth by the primary endpoint, as a reduction
8 in [^{11}C]PiB signal in the PET scans was observed in the control and PBT2 treated groups.
9
10 However, it is noteworthy that like in the EURO study, PBT2 may have reduced the amount of
11 soluble plaque, while not depleting insoluble plaque. Whereas [^{11}C]PiB and the three FDA-
12 approved plaque imaging agents ([^{18}F]AmyvidTM,³⁶⁻³⁷ [^{18}F]NeuraceqTM,³⁸ [^{18}F]VizamylTM³⁹)
13 have become instrumental for PET imaging of neurodegenerative diseases, these compounds are
14 not sensitive enough for early disease detection and are limited by their inability to effectively
15 image soluble and non-fibrillar A β -plaques.⁴⁰⁻⁴² It has also been observed that marked changes in
16 [^{11}C]PiB (and the related approved ^{18}F -agents) retention in AD patients is relatively small which
17 could lead to inconclusive results,⁴³ therefore a A β -plaque imaging radiotracer with higher
18 sensitivity for amyloidosis is still desperately needed for accurate diagnosis and to guide
19 therapeutic trials. A critical point to note is that PBT2 was well-tolerated and safe in the subjects
20 over 52 weeks. Concordant safety and tolerability data were also obtained from Phase II trial of
21 PBT2 in HD patients,⁴⁴ making this lead drug an ideal scaffold for PET radiopharmaceutical
22 development of metallobiology and the “metal hypothesis of AD” *in vivo*.
23
24
25
26
27
28
29
30
31
32
33
34
35
36
37
38
39
40
41
42
43
44

45 Herein, we report the first radiosynthesis of [^{11}C]PBT2 ([^{11}C]7). PET imaging studies with
46 [^{11}C]7 were conducted in rodents and non-human primates. Autoradiography was also
47 performed with human AD brain sections to assess [^{11}C]PBT as a lead compound for clinical
48 translation.
49
50
51
52
53
54
55
56
57
58
59
60

EXPERIMENTAL SECTION

General Methods. All solvents were of reagent or anhydrous grade quality and purchased from Sigma-Aldrich, Alfa Aesar, or Fisher Scientific. All reagents were purchased from Sigma-Aldrich, Alfa Aesar, or Fisher Scientific. ^1H and ^{13}C NMR spectra were recorded on a Bruker 300 MHz spectrometer, and resonances are given in parts per million (ppm) relative residual solvent. Peak multiplicities are designated by the following abbreviations: s, singlet; bs, broad singlet; d, doublet; t, triplet; q, quartet; m, multiplet; dd, doublet of doublets; dt, doublet of triplets; br, broad; and J, coupling constant in Hz. Analytical thin layer chromatography (TLC) was performed on pre-coated glass-backed plates (EMD TLC Silica gel 60 F254) and visualized using a UV lamp (254 nm). HPLC analysis was performed with XSelectTM HSS T3 3.5 μm (4.6 X 150 mm column), 35:65 $\text{CH}_3\text{CN}/0.1\text{N}$ ammonium formate at pH=4 (glacial acetic acid) at a flow rate of 1 mL/min, 8 min run, ultraviolet detection ($\lambda = 254, 224$ nm). All animal procedures were performed in accordance with the National Institutes of Health Guide for the Care and Use of Laboratory Animals and were approved by the Massachusetts General Hospital Institutional Animal Care and Use Facility. Frozen human brain tissue samples (20 μm thick sections) from AD-positive brains were generously provided by Dr. Teresa Gomez-Isla (Massachusetts General Hospital & Harvard Medical School).

Chemistry. *5,7-Dichloro-2-((dimethylamino)methyl)quinolin-8-ol* (PBT2, **7**) A solution of 1.0 M dimethylamine in methanol (1.75 ml, 3.5 mmol) and DIPEA (0.70 ml, 0.6 mmol) were added dropwise slowly to a two-necked flask charged with a solution of *tert*-butyl-(5,7-dichloro-2-formylquinolin-8-yl)carbonate **8** (300 mg, 0.87 mmol) in methanol at room temperature. The resulting reaction mixture was stirred for 2 h at room temperature. Following this, the reaction mixture was cooled to 0 $^\circ\text{C}$ and NaBH_4 (165 mg, 4.3 mmol) was added in portions to the reaction

1
2
3 mixture via one of the openings in the flask, while maintaining N₂ atmosphere. The reaction was
4 slowly warmed to room temperature and stirred for an additional 5h at room temperature. The
5 reaction mixture was slowly quenched with water and saturated sodium bicarbonate solution, and
6 the aqueous layer was extracted with dichloromethane (3 X 15 ml). The combined organic phase
7 was concentrated *in vacuo* to yield the product, 5,7-dichloro-2-
8 ((dimethylamino)methyl)quinolin-8-ol (PBT2, **7**) as a yellow solid in 125 mg (52.5 % isolated
9 yield). Purity > 99% (HPLC λ = 254 nm, HPLC method described in radiochemistry section). ¹H
10 NMR (300 MHz, acetone-*d*₆) δ 8.49(d, *J* = 8.7 Hz, 1H), 7.83(d, *J* = 8.7 Hz, 1H), 7.64(s, 1H), 4.04
11 (br s, 1H (OH)), 3.82 (s, 2H), 2.31 (s, 6H) ; ¹³C NMR (75 MHz, acetone-*d*₆) δ 160.2, 148.7,
12 138.2, 133.4, 127.4, 124.1, 122.7, 119.7, 115.1, 65.1, 44.9. HRMS: calculated 271.0405,
13 observed 271.0399.
14
15
16
17
18
19
20
21
22
23
24
25
26
27
28
29

30 **Radiochemistry.** *Automated Radiosynthesis of [¹¹C]PBT2. [¹¹C]CH₃I synthesis.* [¹¹C]Methyl
31 iodide ([¹¹C]CH₃I) was prepared using a commercially available [¹¹C]CH₃I synthesis apparatus
32 (GE TracerLab FX MeI). In brief, no-carrier-added [¹¹C]carbon dioxide ([¹¹C]CO₂) production
33 was performed using a GEMS PETtrace cyclotron. The ¹⁴N(p, α)¹¹C reaction was employed in a
34 pressurized gas target containing nitrogen (nitrogen 6.0) and 1% oxygen (oxygen 6.0) by
35 bombardment with 50 μ A proton beam for 30 min (~3 Ci of [¹¹C]CO₂). [¹¹C]CO₂ was delivered
36 from the cyclotron target *via* a 1/8" stainless-steel delivery line by nitrogen pressure directly to a
37 column packed with 0.3 g of molecular sieve and 0.2 g of nickel (Shimalite-Ni (reduced),
38 Shimadzu Inc., Kyoto, Japan) where it was trapped at rt. The column was then sealed under
39 hydrogen gas and heated to 350°C for 80 s to reduce the [¹¹C]CO₂ to [¹¹C]CH₄. The [¹¹C]CH₄
40 was passed through a column of phosphorous pentoxide and trapped on a column of carbosphere
41 cooled to -75°C (with liquid nitrogen). Gaseous [¹¹C]CH₄ was released by heating the
42
43
44
45
46
47
48
49
50
51
52
53
54
55
56
57
58
59
60

1
2
3 carbosphere column to 80°C. Once released, the [¹¹C]CH₄ entered a circulation loop, which
4 includes a membrane-based gas pump, a column of iodine at 100°C, a quartz-glass iodine reactor
5 tube at 740°C, two adjacent columns of Ascarite II, and a column of Porapak Q at room
6 temperature. The gaseous mixture was circulated for 5 min, whereas [¹¹C]CH₃I accumulated on
7 the Porapak column. [¹¹C]CH₃I (13.0–37.0 GBq, 350–1000 mCi) was then released from the
8 Porapak column and delivered directly to the reaction vessel using a control stream of He flow
9 (12 mL/min) while heating the Porapak column to 190°C. *Radiotracer Synthesis.* 13.0–37.0
10 GBq (350–1000 mCi) of [¹¹C]CH₃I was delivered to a custom-made 3 mL glassy carbon reaction
11 vessel (Synthra; Part No:00240780) and the corresponding 12 mm reaction vessel head (Synthra;
12 Part No:00224010) and fit to the GE Tracerlab FX_{F-N} containing 0.3 mg of the precursor **9** in a
13 solution of DMSO/DMF (100 μl/200 μl) as solvent in a stream of helium gas at a flow rate of 12
14 ml/min followed by cooling to 50 °C. After the end of radioactivity delivery, the reaction vial
15 was heated at 120°C for 7 min. The reaction was quenched with 1.5 ml of mobile phase and
16 injected onto a HPLC column (XSelect™ HSS T3 Prep 5μm 10 X 250 mm column) and eluted
17 with 35:65 CH₃CN/0.1N ammonium formate at a flow rate of 4 mL/min. The eluent was
18 monitored by UV (λ = 254 nm) and radiochemical detectors connected in series (*R*_t [¹¹C]PBT2 =
19 12.5 minutes). The product was diluted with 25 mL of sterile water. The diluted HPLC fraction
20 was then loaded on an Oasis HLB light cartridge, then washed with 10 mL sterile water.
21 [¹¹C]PBT2 was recovered in 1.0 mL dehydrated ethanol for injection, USP, and 10 mL of 0.9%
22 sodium chloride for injection, USP. [¹¹C]PBT2 was obtained in 4.80 ± 0.45 % radiochemical
23 yields (RCYs) (s.d., non-decay corrected) radiochemical yields (RCYs) at end-of-synthesis (~ 50
24 min) based upon [¹¹C]CH₃I (*n* = 6), with > 99% radiochemical purity and 80-90 GBq/μmol
25 molar activity (*A*_m). Product identity and purity were determined by radio-HPLC (35:65
26
27
28
29
30
31
32
33
34
35
36
37
38
39
40
41
42
43
44
45
46
47
48
49
50
51
52
53
54
55
56
57
58
59
60

1
2
3 CH₃CN: 0.1 N ammonium formate at pH 4 (acetic acid), XSelect™ HSS T3 column) and UV
4
5 by co-injection with the standard.
6
7

8
9 **Small Animal PET Imaging in mice.** BALB/c mice ($n = 2, 24$ and 30 g, COX7) were serially
10
11 imaged dynamically using a Sofie G4 small animal PET scanner (frames \times min: $2 \times 0.5, 5 \times 1, 2$
12
13 $\times 12, 1 \times 30$). For all imaging experiments, mice were anesthetized using 2% isoflurane in O₂ at
14
15 a flow rate of ~ 1.5 L/min, positioned in a prone position along the long axis of the PET scanner
16
17 and imaged. Images were reconstructed using a filtered back projection reconstruction algorithm.
18
19 For image analysis, regions of interest (ROIs) were manually drawn from three-dimensional
20
21 filtered back projection (FBP) reconstructed PET images using AMIDE software. Regional
22
23 radioactivity was expressed as the percentage standardized uptake value [% SUV = % ID/mL \times
24
25 body weight (g)].
26
27

28
29 **NHP PET/MRI Imaging.** A female Papio anubis baboon (8 years, 14 kg), deprived of food for
30
31 12 h prior to the study, was administered intramuscular ketamine (10 mg/kg) and intubated. For
32
33 maintenance of anesthesia throughout the study, the baboon was provided 1 – 4% isoflurane
34
35 (Forane) in a mixture of medical oxygen and nitrogen. The baboon was catheterized
36
37 antecubitally for radiotracer injection. PET-MR acquisition was performed on a 3T Siemens
38
39 TIM-Trio with a BrainPET insert (Siemens, Erlangen, Germany). A PET/MRI compatible eight-
40
41 channel array coil customized for nonhuman primate brain imaging was utilized. Dynamic PET
42
43 image acquisition was initiated followed by administration of the radiotracer (5.2 mCi) in a
44
45 homogenous solution of 10% ethanol and 90% isotonic saline. An MEMPRAGE sequence was
46
47 initiated for anatomic co-registration. Dynamic data from the PET scans were recorded in list
48
49 mode for 90 min. Images were reconstructed using the 3D ordinary Poisson expectation
50
51 maximization algorithm with detector efficiency, decay, dead time, attenuation, and scatter
52
53
54
55
56
57
58
59
60

1
2
3 corrections. PET data was binned in 26 frames (6 X 10 s, 6 X 20 s, 2 X 30 s, 1 X 60s, 5 X 300 s,
4
5 6 X 600 s) and image volumes were reconstructed into 76 slices with 128 x 128 pixels and a 2.5
6
7 mm isotropic voxel size. PET data was coregistered to the Black baboon brain atlas using JIP
8
9 tools optimized for nonhuman primate data processing (www.nitrc.org/projects/jip). Image
10
11 registration was carried out on high- resolution T1-weighted anatomical MRI images using a 12
12
13 degree of freedom linear algorithm and a nonlinear algorithm to the atlas brain. The
14
15 transformation was then applied to the simultaneously collected dynamic PET data. PET data
16
17 analysis was performed using PMOD 3.3 (PMOD Technologies Ltd., Zurich, Switzerland).
18
19 Fifteen volumes of interest (VOIs) were defined per the Black baboon brain atlas. Time–activity
20
21 curves (TACs) were extracted from the anterior cingulate cortex (ACC), amygdala (Amyg),
22
23 caudate (Cau), cerebellum (CB), dorsal lateral prefrontal cortex (DLPFC), hippocampus (HIP),
24
25 primary motor cortex (M1), nucleus accumbens (NAc), orbitofrontal cortex (OFC), posterior
26
27 cingulate cortex (PCC), primary visual cortex (V1), putamen (Put), supplementary motor area
28
29 (SMA), thalamus (Tha), whole brain (WM), VOIs for analysis. Symmetrical structures were
30
31 averaged before further analysis. For SUV calculations, time points between 0 and 90 min were
32
33 averaged for each VOI.
34
35
36
37
38
39
40
41
42

43 **Autoradiography.** Brain tissue was provided by Dr. Matthew Froesch from the Neuropathology
44
45 Core at the Massachusetts Alzheimer's Disease Research Center. Baseline and blocking
46
47 experiments were performed on adjacent sections. On the day of the synthesis, sections were
48
49 thawed at room temperature, air dried followed by pre-incubation in 50 mM Tris HCl buffer (pH
50
51 7.4) for 30 min. Tissue was then incubated with 0.2 MBq/ml (5 μ Ci/ml) of [11 C]PBT2 alone
52
53 (baseline) or [11 C]PBT2 in the presence of 10 μ M PBT2 (blocking) in the same buffer solution at
54
55
56
57
58
59
60

1
2
3 room temperature for 30 min. After incubation, slides were washed twice in buffer (4°C, 5 min
4 each) followed by rinsing one time in distilled water and dried subsequently. The sections were
5 then exposed on a radioluminographic imaging plate (PerkinElmer 7001723) for 1 h following
6 which autoradiography images were obtained with a Cyclone Plus Storage Phosphor
7 (PerkinElmer) detector. Activity in photostimulated luminescence unit per mm² was calculated
8 for each ROI using ImageJ. Gray and white matter binding are averaged.
9
10
11
12
13
14
15
16
17
18
19

20 RESULTS AND DISCUSSION

21
22 The normethyl precursor 5,7-dichloro-2-((methylamino)methyl)quinolin-8-ol (**9**, **Scheme 1B**),
23 for the synthesis of [¹¹C]PBT2 was prepared as previously described in 4-steps from
24 commercially available materials.⁴⁵ Authentic PBT2 (**7**) was synthesized as the free amine by
25 modifying a previously reported protocol from boc-protected aldehyde **8** using dimethylamine in
26 52% isolated yield (**Scheme 1A**).^{26, 28} Carbon-11 labeled PBT2 ([¹¹C]**7**, **Figure 1B**) was
27 synthesized by reaction of [¹¹C]CH₃I with **9** via an automated method, which uses the GE
28 TracerLab_{FXM} module for [¹¹C]CH₃I production and a modified small-volume glass vial (custom
29 manufactured by Synthra) designed to fit the commercial radiofluorination module (GE
30 Tracerlab FX_{F-N}) which was connected in series for purification and formulation. This vial
31 allows the use of a traditional automated radiofluorination apparatus for small-volume carbon-11
32 labeling reactions. Radiolabeling was performed in a mixture of DMF and DMSO (2:1, v/v)
33 for 7 min at 120 °C which led to the isolation of [¹¹C]PBT2 in 4.8 ± 0.5% (s.d., *n* = 6) RCYs,
34 >99% radiochemical purity with *A_m* of 80-90 GBq/μmol (2200-2500 mCi/μmol), which is
35 consistent with non-decay corrected RCYs of most ¹¹C-labeled PET radiopharmaceuticals. This
36 automated synthesis allows for the large-scale production of [¹¹C]PBT2 (starting with 37.0 GBq
37
38
39
40
41
42
43
44
45
46
47
48
49
50
51
52
53
54
55
56
57
58
59
60

1
2
3 (1 Ci) of [^{11}C]CH₃I) to enable advanced preclinical PET imaging studies. We anticipate that
4
5 this radiosynthesis would be suitable for validation of [^{11}C]PBT2 and clinical translation would
6
7 be further simplified as PBT2 has been shown to be safe and well-tolerated in human based on
8
9 reported Phase II trial outcomes,^{33,44} therefore toxicity studies would not be required for this ^{11}C -
10
11 isotopolog.
12
13

14
15 We performed [^{11}C]PBT2 imaging studies in BALB/c mice and non-human primates and
16
17 preliminary *in vitro* autoradiography studies using human AD brain tissue with the aim of
18
19 clarifying three major requirements in support of the tracer's translation towards human PET
20
21 studies, specifically: defining whether or not [^{11}C]PBT2 displays (i) sufficient brain exposure,
22
23 (ii) favorable brain pharmacokinetics *in vivo* and (iii) saturable binding to AD brain tissue *in*
24
25 *vitro*.
26
27
28
29

30
31
32
33
34
35
36
37
38
39
40
41
42
43
44
45
46
47
48
49
50
51
52
53
54
55
56
57
58
59
60
Insert Scheme 1

Dynamic small animal PET imaging data were acquired for 30 min and demonstrated that
[^{11}C]PBT2 rapidly permeates the blood-brain barrier (BBB) in mice following intravenous
injection with peak SUV for the whole brain (SUV_{peak}) of 1.3 ± 0.3 (at 1.3 min post-injection, n
= 2, **Figure 2**). The initial uptake was followed by fast washout of the radiotracer with
SUV_{peak}/SUV_{30 min} ratio of 6.3 and only negligible radioactivity remaining in the brain in the later
phase (20-30 min post-injection). The data presented here with regard to [^{11}C]PBT2 brain
exposure and clearance were analogous to the trends observed in rodents with [^{18}F]CABS13 but
favorable compared to previously described data for the SPECT radiotracer [^{125}I]CQ.^{20-21, 23}

Insert Figure 2

1
2
3 Carbon-11 labeled PBT2 displayed excellent brain penetration in the non-human primate
4 brain following intravenous injection (**Figure 3**). Brain uptake at SUV_{peak} and in the early phase
5 (0-20 min) was high and heterogeneous with an averaged SUV_{peak} in gray matter areas of 4.09 at
6 2.2-4.5 min post-injection and most pronounced in the caudate and putamen (4.57-5.05) while
7 subcortical white matter was associated with lowest uptake (2.33 SUV_{peak} @ 4.5 post-injection)
8 (**Figure 4**). This initial uptake was followed by a favorable and fast brain tissue clearance with
9 convergence of all time-activity curves and uniform kinetics for all brain regions, including
10 subcortical white matter, starting 25 min post-injection throughout the remainder 90 min
11 scanning time and is in accordance with an absence of pathological metal-concentrated
12 peptide/protein aggregates (**Figure 4, Figure S3**). The *in vivo* profile of [^{11}C]PBT2 in primate is
13 in contrast with the clinical SPECT results obtained with [^{125}I]CQ as well as the preclinical
14 primate data from the evaluation of [^{18}F]CABS13 – both radiotracers were deemed to be
15 unsuitable for neuroimaging based on negligible CNS uptake.
16
17
18
19
20
21
22
23
24
25
26
27
28
29
30
31
32

33 Importantly, the primate PET data presented here suggest that the lack of efficacy seen in
34 the IMAGINE/extension trial in AD patients (NCT:00471211) likely does not originate from a
35 lack of CNS drug exposure.³³ These recently reported clinical results may be related to the
36 propensity of the tridentate PBT2 to form ternary complexes, including PBT2-Cu^{II}-A β , which
37 prevent proper clearance and/or redistribution of aggregated metal.⁴⁶⁻⁴⁷ The rapid washout seen
38 here in NHP after high initial brain permeation also indicates that [^{11}C]PBT2 does not form
39 intracellularly trapped ternary complex (under non-pathological condition) or CNS-retained
40 metabolites. Prana Biotechnology has studied PBT2 and [^{14}C]PBT2 in phase I trials and showed
41 that the drug was primarily metabolized as its PBT2-glucuronide and renally excreted.⁴⁸ The
42 formation of such polar [^{11}C]PBT2-glucuronide primary metabolite is not expected to cross the
43
44
45
46
47
48
49
50
51
52
53
54
55
56
57
58
59
60

1
2
3 BBB or otherwise interfere with the CNS [¹¹C]PBT2 PET signal or quantification in present and
4
5
6
7
8
9
10
11
12
13
14
15
16
17
18
19
20
21
22
23
24
25
26
27
28
29
30
31
32
33
34
35
36
37
38
39
40
41
42
43
44
45
46
47
48
49
50
51
52
53
54
55
56
57
58
59
60

BBB or otherwise interfere with the CNS [¹¹C]PBT2 PET signal or quantification in present and upcoming studies. It is important to note that whether or not PBT2 will prove efficacious in any further Phase II/III trials for AD or HD will need to be assessed independently of the question of the potential use of [¹¹C]PBT2 as a PET radiotracer to study metallobiology in neurodegenerative diseases. The putative mechanistic limitation of PBT2 as a drug (e.g. preferential ternary complex formation over 2:1 complex which could enable therapeutic metal redistribution) will not likely impact the application of [¹¹C]PBT2 under the inherent microdosing conditions used in PET. In light of the promising *in vivo* PET imaging profiles observed with this radiotracer, we carried out autoradiography studies and confirmed that [¹¹C]PBT2 binds specifically to postmortem AD human brain cryosections (occipital cortex; $\Delta = -36.2 \pm 2.7\%$ following self-blocking conditions, **Figure S4**).

Insert Figure 3

Insert Figure 4

39
40
41
42
43
44
45
46
47
48
49
50
51
52
53
54
55
56
57
58
59
60

Taken together, the extensive [¹¹C]PBT2 brain uptake and rapid subsequent washout observed here in primate, combined with the safety, tolerability and favorable metabolic profiles of PBT2 established in human have provided an accelerated path to [¹¹C]PBT2 human PET studies. In particular, we anticipate that the high striatal sensitivity of [¹¹C]PBT2 may prove useful beyond AD, for example in studying the role of metal accumulation in striatal degeneration in HD patients.^{30, 49} Detailed quantification, radiometabolite assessments and human PET evaluation will be reported in a separate account.

1
2
3
4
5
6
7
8
9
10
11
12
13
14
15
16
17
18
19
20
21
22
23
24
25
26
27
28
29
30
31
32
33
34
35
36
37
38
39
40
41
42
43
44
45
46
47
48
49
50
51
52
53
54
55
56
57
58
59
60

FIGURE LEGENDS

Figure 1. Chemical structures of representative metal protein attenuating compounds (MPACs), metal chelators and corresponding reported SPECT/PET radiotracers.

Figure 2. TAC for [^{11}C]PBT2 uptake in mice brain at baseline (whole brain; expressed as mean \pm SD; $n = 2$)

Figure 3. *In vivo* PET imaging of [^{11}C]PBT2 in the non-human primate brain. Coronal, sagittal and transverse MRI, summed PET and overlaid images (5-15 min and 60-90 min p.i.) of [^{11}C]PBT2 in the baboon (*Papio anubis*) brain.

Figure 4. Regional [^{11}C]PBT2 TACs in the non-human primate brain. CRB, cerebellum; HIP, hippocampus; PUT, putamen; THA, thalamus; CAUD, caudate; WM, white matter; CTX, cortex.

FIGURES

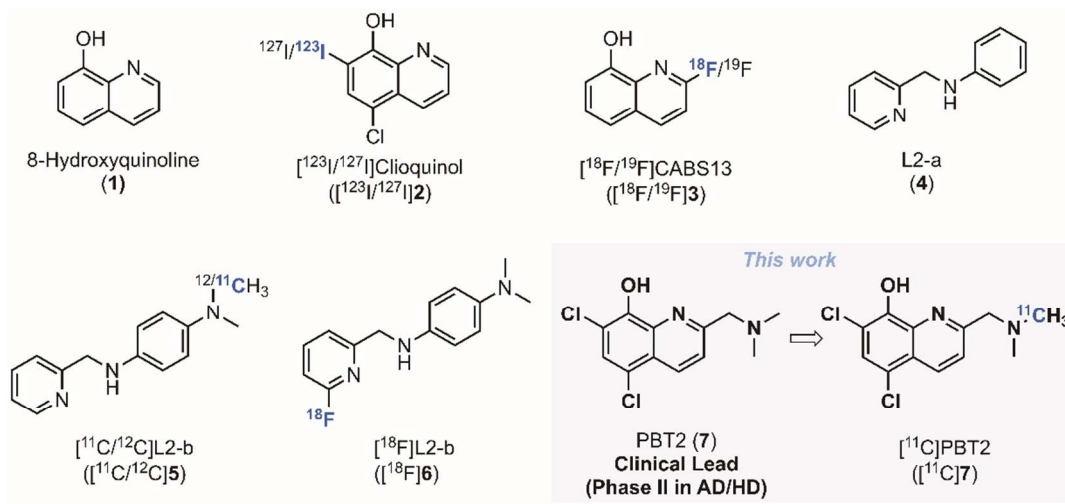


Figure 1. Chemical structures of representative metal protein attenuating compounds, metal chelators and corresponding reported SPECT/PET radiotracers.

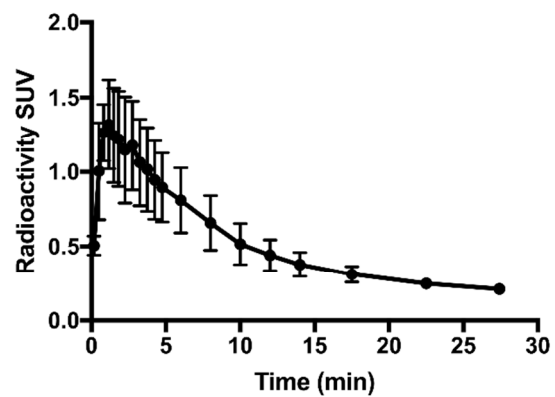
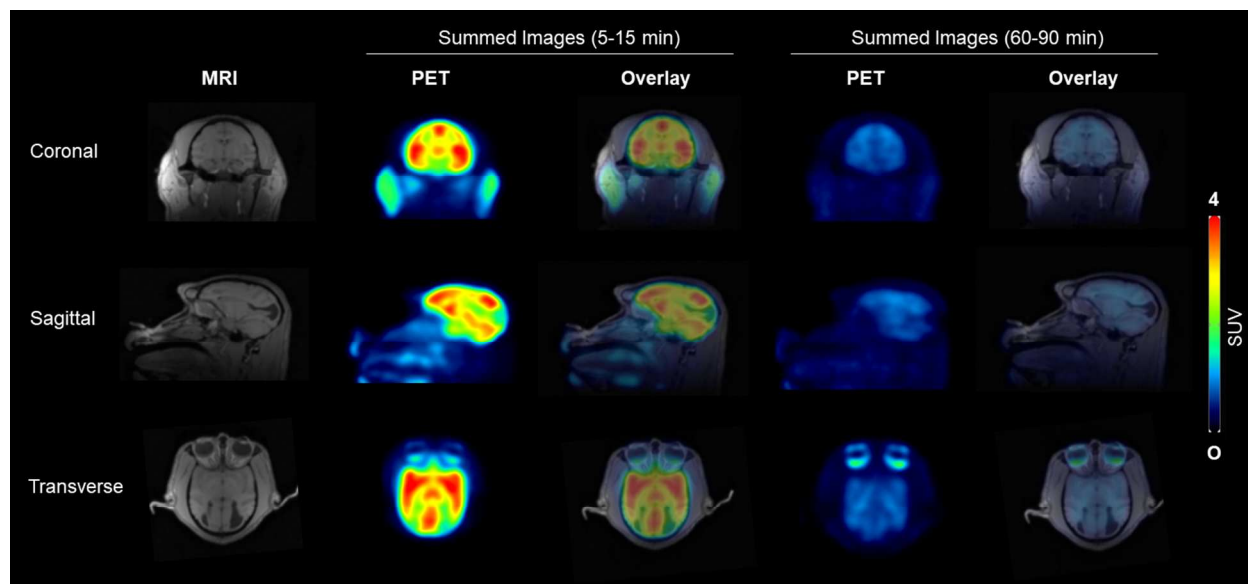


Figure 2. Time-activity curve of $[^{11}\text{C}]$ PBT2 uptake in mouse brain at baseline (whole brain; expressed as mean \pm SD; $n = 2$)



22
23
24
25
26
27
28
29
30
31
32
33
34
35
36
37
38
39
40
41
42
43
44
45
46
47
48
49
50
51
52
53
54
55
56
57
58
59
60

Figure 3. *In vivo* PET imaging of [¹¹C]PBT2 in the non-human primate brain. Coronal, sagittal and transverse MRI, summed PET and overlaid images (5-15 min and 60-90 min p.i.) of [¹¹C]PBT2 in the baboon (*Papio anubis*) brain.

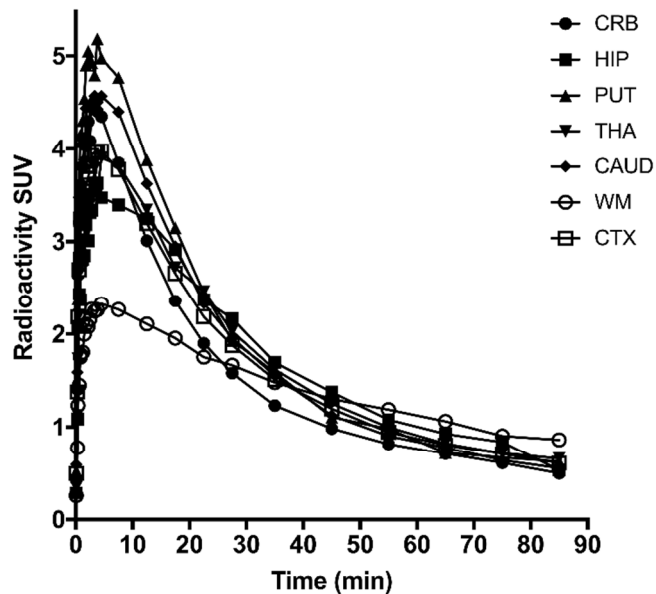
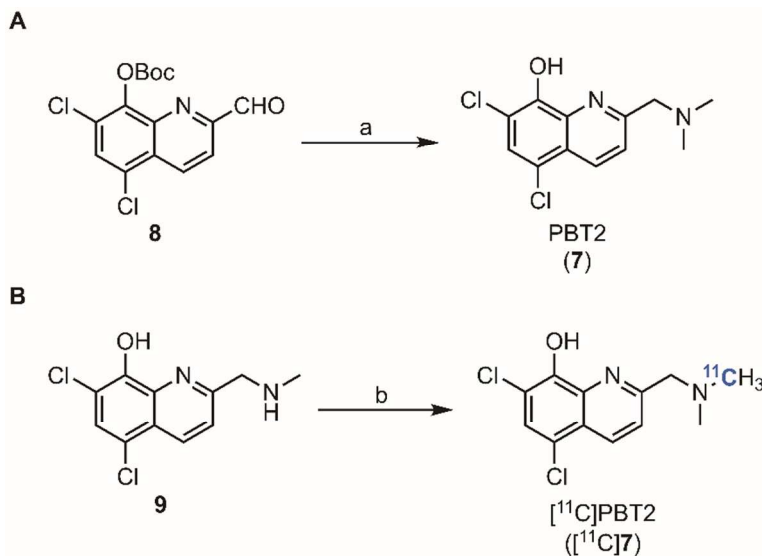


Figure 4. Regional [¹¹C]PBT2 TACs in the non-human primate brain. CRB, cerebellum; HIP, hippocampus; PUT, putamen; THA, thalamus; CAUD, caudate; WM, white matter; CTX, cortex.

SCHEMES

Scheme 1. Synthesis of PBT2 and radiosynthesis of [¹¹C]PBT2 from the corresponding normethyl precursor^a

^aReagents and conditions: (a) Me₂NH (5 equiv.), MeOH, rt, 2 h, then NaBH₄, MeOH, 5 h (isolated yield = 52.5 %); (b) [¹¹C]CH₃I, DMSO/DMF (1:2), 7 min, 120°C; (isolated RCY = 4.8 ± 0.5%)

1
2
3 ASSOCIATED CONTENT
4
5

6 ^1H and ^{13}C NMR of PBT2, Figure S1. HPLC chromatogram formulated [^{11}C]PBT2 (coinjecting
7 with PBT2), Figure S2. Detailed regional TACs of [^{11}C]PBT2 in nonhuman primate, Figure S3.
8
9 Binding of [^{11}C]PBT2 in postmortem human tissue, Figure S4. This material is available free of
10
11 charge via the Internet at <http://pubs.acs.org>.
12
13
14
15

16 AUTHOR INFORMATION
17

18
19 **Corresponding Author**
20

21
22 *For N.V.: E-mail, vasdev.neil@mgh.harvard.edu / phone, +1-617-643-4736
23
24

25
26 *For S.H.L.: E-mail, liang.steven@mgh.harvard.edu / phone, +1 617 726 6106
27
28

29 **Author Contributions**
30

31 The manuscript was written through contributions of all authors. All authors have given approval
32
33 to the final version of the manuscript.
34
35
36
37
38
39
40
41
42
43
44
45
46
47
48
49
50
51
52
53
54
55
56
57
58
59
60

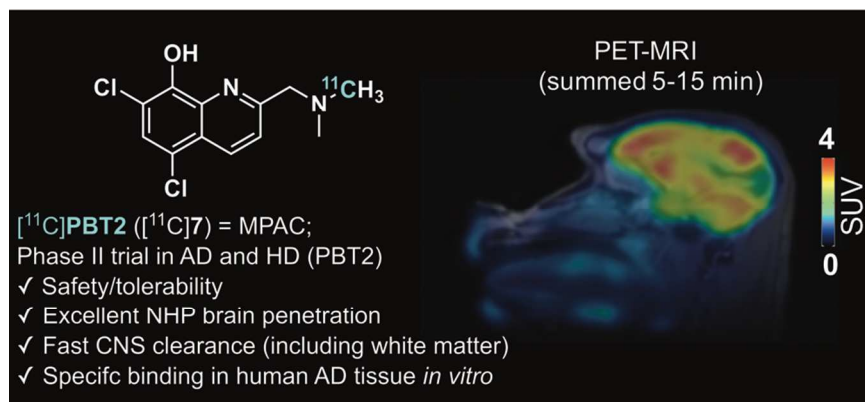
ACKNOWLEDGMENTS

We thank David F. Lee, Jr., for radioisotope production. We thank Dr. Teresa Gomez-Isla for generously providing human brain sections for autoradiography. We are grateful to Dr. Longle Ma, Baileigh Hightower, Shirley Hsu, Grae Arabasz, and Helen Deng for assistance with the PET/MR NHP imaging experiment, and Dr. Ramesh Neelamegam, and Mo Farhoud for helpful discussions and technical assistance. We thank Dr. Bruno Nebeling, Synthra GmbH for providing us with the small reaction vessel used to modify the existing GE FXN module. We thank Marilyn Grand'Maison for assistance with figure preparations. S.H.L. is a recipient of a NIH career development award from the National Institute on Drug Abuse (DA038000) and N.V. thanks National Institute on Ageing of the NIH (R01AG054473) for support.

ABBREVIATIONS

A β , amyloid- β ; AD, Alzheimer's disease; BBB, blood-brain barrier; CQ, clioquinol; DMF, *N,N*-dimethylformamide; DMSO, dimethyl sulfoxide; [18 F]FDG, 2-deoxy-2-[18 F]fluoroglucose; HD, Huntington's disease; MRI, magnetic resonance imaging; MPAC, metal protein-attenuating compound; PiB, Pittsburgh compound B; PET, positron emission tomography; SD, standard deviation; SPECT, single photon emission computed tomography; SUV, standardized uptake value; TAC, time activity curve.

TOC



REFERENCES

1. Abbott, A., Dementia: a problem for our age. *Nature* **2011**, *475* (7355), S2-4.
2. Jakob-Roetne, R.; Jacobsen, H., Alzheimer's Disease: From Pathology to Therapeutic Approaches. *Angew. Chem., Int. Ed.* **2009**, *48* (17), 3030-3059.
3. Greenough, M. A.; Camakaris, J.; Bush, A. I., Metal dyshomeostasis and oxidative stress in Alzheimer's disease. *Neurochemistry International* **2013**, *62* (5), 540-555.
4. Rauk, A., The chemistry of Alzheimer's disease. *Chem. Soc. Rev.* **2009**, *38* (9), 2698-2715.
5. James, S. A.; Volitakis, I.; Adlard, P. A.; Duce, J. A.; Masters, C. L.; Cherny, R. A.; Bush, A. I., Elevated labile Cu is associated with oxidative pathology in Alzheimer disease. *Free Radical Biol. Med.* **2012**, *52* (2), 298-302.
6. Faller, P.; Hureau, C., Bioinorganic chemistry of copper and zinc ions coordinated to amyloid- β peptide. *Dalton Trans.* **2009**, (7), 1080-1094.
7. Gaggelli, E.; Kozlowski, H.; Valensin, D.; Valensin, G., Copper homeostasis and neurodegenerative disorders (Alzheimer's, prion, and Parkinson's diseases and amyotrophic lateral sclerosis). *Chem. Rev. (Washington, DC, U. S.)* **2006**, *106* (6), 1995-2044.
8. Bush, A. I.; Tanzi, R. E., Therapeutics for Alzheimer's disease based on the metal hypothesis. *Neurotherapeutics* **2008**, *5* (3), 421-432.
9. Ayton, S.; Lei, P.; Bush, A. I., Metallostasis in Alzheimer's disease. *Free Radical Biol. Med.* **2013**, *62*, 76-89.
10. Mason, R. P.; Casu, M.; Butler, N.; Breda, C.; Campesan, S.; Clapp, J.; Green, E. W.; Dhulkhed, D.; Kyriacou, C. P.; Giorgini, F., Glutathione peroxidase activity is neuroprotective in models of Huntington's disease. *Nat. Genet.* **2013**, *45* (10), 1249-1254.
11. Valentine, J. S.; Hart, P. J., Misfolded CuZnSOD and amyotrophic lateral sclerosis. *Proc. Natl. Acad. Sci. U. S. A.* **2003**, *100* (7), 3617-3622.
12. Rasia, R. M.; Bertoncini, C. W.; Marsh, D.; Hoyer, W.; Cherny, D.; Zweckstetter, M.; Griesinger, C.; Jovin, T. M.; Fernandez, C. O., Structural characterization of copper(II) binding to α -synuclein: insights into the bioinorganic chemistry of Parkinson's disease. *Proc. Natl. Acad. Sci. U. S. A.* **2005**, *102* (12), 4294-4299.
13. Hands, S. L.; Mason, R.; Sajjad, M. U.; Giorgini, F.; Wytenbach, A., Metallothioneins and copper metabolism are candidate therapeutic targets in Huntington's disease. *Biochem. Soc. Trans.* **2010**, *38* (2), 552-558.
14. Crouch, P. J.; Barnham, K. J., Therapeutic Redistribution of Metal Ions To Treat Alzheimer's Disease. *Acc. Chem. Res.* **2012**, *45* (9), 1604-1611.
15. Bareggi, S. R.; Cornelli, U., Clioquinol: review of its mechanisms of action and clinical uses in neurodegenerative disorders. *CNS Neurosci. Ther.* **2012**, *18* (1), 41-46.
16. Cherny, R. A.; Atwood, C. S.; Xilinas, M. E.; Gray, D. N.; Jones, W. D.; McLean, C. A.; Barnham, K. J.; Volitakis, I.; Fraser, F. W.; Kim, Y.-S.; Huang, X.; Goldstein, L. E.; Moir, R. D.; Lim, J. T.; Beyreuther, K.; Zheng, H.; Tanzi, R. E.; Masters, C. L.; Bush, A. I., Treatment with a Copper-Zinc Chelator Markedly and Rapidly Inhibits β -Amyloid Accumulation in Alzheimer's Disease Transgenic Mice. *Neuron* **2001**, *30* (3), 665-676.
17. <http://www.alzforum.org/therapeutics/cliouinol>.
18. Ibach, B.; Haen, E.; Marienhagen, J.; Hajak, G., Clioquinol Treatment in Familiar Early Onset of Alzheimer's Disease. *Pharmacopsychiatry* **2005**, *38* (04), 178-179.

19. Papazian, V.; Jackson, T.; Pham, T.; Liu, X.; Greguric, I.; Loc'h, C.; Rowe, C.; Villemagne, V.; Masters, C. L.; Katsifis, A., The preparation of 123/125I-clioquinol for the study of A β protein in Alzheimer's disease. *J. Labelled Compd. Radiopharm.* **2005**, *48* (7), 473-484.
20. Opazo, C.; Luza, S.; Villemagne, V. L.; Volitakis, I.; Rowe, C.; Barnham, K. J.; Strozzyk, D.; Masters, C. L.; Cherny, R. A.; Bush, A. I., Radioiodinated clioquinol as a biomarker for β -amyloid: Zn²⁺ complexes in Alzheimer's disease. *Aging Cell* **2006**, *5* (1), 69-79.
21. Vasdev, N.; Cao, P.; van Oosten, E. M.; Wilson, A. A.; Houle, S.; Hao, G.; Sun, X.; Slavine, N.; Alhasan, M.; Antich, P. P.; Bonte, F. J.; Kulkarni, P., Synthesis and PET imaging studies of [18F]2-fluoroquinolin-8-ol ([18F]CABS13) in transgenic mouse models of Alzheimer's disease. *MedChemComm* **2012**, *3* (10), 1228-1230.
22. Liang, S. H.; Collier, T. L.; Rotstein, B. H.; Lewis, R.; Steck, M.; Vasdev, N., Rapid microfluidic flow hydrogenation for reduction or deprotection of 18F-labeled compounds. *Chem. Commun. (Cambridge, U. K.)* **2013**, *49* (78), 8755-8757.
23. Liang, S. H.; Holland, J. P.; Stephenson, N. A.; Kassenbrock, A.; Rotstein, B. H.; Daignault, C. P.; Lewis, R.; Collier, L.; Hooker, J. M.; Vasdev, N., PET Neuroimaging Studies of [18F]CABS13 in a Double Transgenic Mouse Model of Alzheimer's Disease and Nonhuman Primates. *ACS Chem. Neurosci.* **2015**, *6* (4), 535-541.
24. Choi, J.-S.; Braymer, J. J.; Nanga, R. P. R.; Ramamoorthy, A.; Lim, M. H., Design of small molecules that target metal-A β species and regulate metal-induced A β aggregation and neurotoxicity. *Proceedings of the National Academy of Sciences* **2010**, *107* (51), 21990-21995.
25. Cary, B. P.; Brooks, A. F.; Fawaz, M. V.; Shao, X.; Desmond, T. J.; Carpenter, G. M.; Sherman, P.; Quesada, C. A.; Albin, R. L.; Scott, P. J. H., Targeting Metal-A β Aggregates with Bifunctional Radioligand [11C]L2-b and a Fluorine-18 Analogue [18F]FL2-b. *ACS Medicinal Chemistry Letters* **2015**, *6* (2), 112-116.
26. Barnham, K. J.; Gautier, E. C. L.; Kok, G. B.; Krippner, G. Preparation of 8-hydroxyquinolines for treatment of neurological conditions. WO2004007461A1, 2004.
27. Bush, A. I., Drug Development Based on the Metals Hypothesis of Alzheimer's Disease. *Journal of Alzheimer's Disease* **2008**, *15* (2), 223-240.
28. Barnham, K. J.; Gautier, E. C. L.; Kok, G. B.; Krippner, G. Preparation of 8-hydroxyquinolines for treatment of neurological conditions. US20080161353A1, 2008.
29. Cherny, R. A.; Ayton, S.; Bush, A. I.; McColl, G.; Finkelstein, D. I.; Massa, S. M., PBT2 Reduces Toxicity in a *C. elegans* Model of polyQ Aggregation and Extends Lifespan, Reduces Striatal Atrophy and Improves Motor Performance in the R6/2 Mouse Model of Huntington's Disease. *J Huntington's Dis* **2012**, *1* (2), 211-9.
30. Fox, J. H.; Kama, J. A.; Lieberman, G.; Chopra, R.; Dorsey, K.; Chopra, V.; Volitakis, I.; Cherny, R. A.; Bush, A. I.; Hersch, S., Mechanisms of Copper Ion Mediated Huntington's Disease Progression. *PLOS ONE* **2007**, *2* (3), e334.
31. Adlard, P. A.; Bica, L.; White, A. R.; Nurjono, M.; Filiz, G.; Crouch, P. J.; Donnelly, P. S.; Cappai, R.; Finkelstein, D. I.; Bush, A. I., Metal Ionophore Treatment Restores Dendritic Spine Density and Synaptic Protein Levels in a Mouse Model of Alzheimer's Disease. *PLOS ONE* **2011**, *6* (3), e17669.
32. Faux, N. G.; Ritchie, C. W.; Gunn, A.; Rembach, A.; Tsatsanis, A.; Bedo, J.; Harrison, J.; Lannfelt, L.; Blennow, K.; Zetterberg, H.; Ingelsson, M.; Masters, C. L.; Tanzi, R. E.; Cummings, J. L.; Herd, C. M.; Bush, A. I., PBT2 Rapidly Improves Cognition in Alzheimer's Disease: Additional Phase II Analyses. *J. Alzheimer's Dis.* **2010**, *20* (2), 509-516.

- 1
2
3 33. Lannfelt, L.; Blennow, K.; Zetterberg, H.; Batsman, S.; Ames, D.; Harrison, J.; Masters,
4 C. L.; Targum, S.; Bush, A. I.; Murdoch, R.; Wilson, J.; Ritchie, C. W., Safety, efficacy, and
5 biomarker findings of PBT2 in targeting A β as a modifying therapy for Alzheimer's disease: a
6 phase IIa, double-blind, randomised, placebo-controlled trial. *The Lancet Neurology* **2008**, *7* (9),
7 779-786.
- 8
9 34. Crouch, P. J.; Savva, M. S.; Hung, L. W.; Donnelly, P. S.; Mot, A. I.; Parker, S. J.;
10 Greenough, M. A.; Volitakis, I.; Adlard, P. A.; Cherny, R. A.; Masters, C. L.; Bush, A. I.;
11 Barnham, K. J.; White, A. R., The Alzheimer's therapeutic PBT2 promotes amyloid- β
12 degradation and GSK3 phosphorylation via a metal chaperone activity. *Journal of*
13 *Neurochemistry* **2011**, *119* (1), 220-230.
- 14
15 35. <http://www.alzforum.org/news/research-news/pbt2-takes-dive-phase-2-alzheimers-trial>.
- 16 36. Wong, D. F.; Rosenberg, P. B.; Zhou, Y.; Kumar, A.; Raymont, V.; Ravert, H. T.;
17 Dannals, R. F.; Nandi, A.; Brasic, J. R.; Ye, W.; Hilton, J.; Lyketsos, C.; Kung, H. F.; Joshi, A.
18 D.; Skovronsky, D. M.; Pontecorvo, M. J., In vivo imaging of amyloid deposition in Alzheimer
19 disease using the radioligand 18F-AV-45 (Florbetapir F 18). *J. Nucl. Med.* **2010**, *51* (6), 913-920.
- 20 37. Doraiswamy, P. M.; Sperling, R. A.; Johnson, K.; Reiman, E. M.; Wong, T. Z.; Sabbagh,
21 M. N.; Sadowsky, C. H.; Fleisher, A. S.; Carpenter, A.; Joshi, A. D.; Lu, M.; Grundman, M.;
22 Mintun, M. A.; Skovronsky, D. M.; Pontecorvo, M. J.; Duara, R.; Sabbagh, M.; Ahern, G. L.;
23 Holub, R. F.; Farmer, M. V.; Safirstein, B. E.; Alva, G.; Longmire, C. F.; Jewell, G.; Johnson, K.
24 A.; Korn, R.; Reiman, E. M.; Wendt, J. K.; Wong, D.; Doraiswamy, P. M.; Coleman, R. E.;
25 Devous, M.; Jennings, D.; Weiner, M. W.; Murphy, C. A.; Kovnat, K. D.; Williamson, J. D.;
26 Sadowsky, C. H., Florbetapir F 18 amyloid PET and 36-month cognitive decline: a prospective
27 multicenter study. *Mol. Psychiatry* **2014**, *19* (9), 1044-1051.
- 28
29 38. Richards, D.; Sabbagh, M. N., Florbetaben for PET Imaging of Beta-Amyloid Plaques in
30 the Brain. *Neurol Ther* **2014**, *3* (2), 79-88.
- 31
32 39. Nelissen, N.; van Laere, K.; Thurfjell, L.; Owenius, R.; Vandenbulcke, M.; Koole, M.;
33 Bormans, G.; Brooks, D. J.; Vandenberghe, R., Phase 1 study of the Pittsburgh compound B
34 derivative 18F-flutemetamol in healthy volunteers and patients with probable Alzheimer disease.
35 *J. Nucl. Med.* **2009**, *50* (8), 1251-1259.
- 36
37 40. Vlassenko, A. G.; Benzinger, T. L. S.; Morris, J. C., PET amyloid-beta imaging in
38 preclinical Alzheimer's disease. *Biochimica et Biophysica Acta (BBA) - Molecular Basis of*
39 *Disease* **2012**, *1822* (3), 370-379.
- 40 41. Mathis, C. A.; Wang, Y.; Holt, D. P.; Huang, G.-F.; Debnath, M. L.; Klunk, W. E.,
41 Synthesis and Evaluation of 11C-Labeled 6-Substituted 2-Arylbenzothiazoles as Amyloid
42 Imaging Agents. *J. Med. Chem.* **2003**, *46* (13), 2740-2754.
- 43 42. Klunk, W. E.; Mathis, C. A., The future of amyloid-beta imaging: a tale of radionuclides
44 and tracer proliferation. *Curr Opin Neurol* **2008**, *21* (6), 683-7.
- 45 43. Jack, C. R., Jr.; Lowe, V. J.; Weigand, S. D.; Wiste, H. J.; Senjem, M. L.; Knopman, D.
46 S.; Shiung, M. M.; Gunter, J. L.; Boeve, B. F.; Kemp, B. J.; Weiner, M.; Petersen, R. C., Serial
47 PIB and MRI in normal, mild cognitive impairment and Alzheimer's disease: implications for
48 sequence of pathological events in Alzheimer's disease. *Brain* **2009**, *132* (Pt 5), 1355-65.
- 49
50 44. Angus, D.; Herd, C.; Stone, C.; Stout, J.; Wieler, M.; Reilmann, R.; Ritchie, C. W.;
51 Dorsey, E. R.; Helles, K.; Kayson, E.; Oakes, D.; Rosas, H. D.; Vaughan, C.; Panegyrs, P. K.;
52 Ames, D.; Goh, A.; Agarwal, P.; Churchyard, A.; Murathodizic, M.; Chua, P.; Germaine, D.;
53 Lim, L.; Mack, H.; Loy, C.; Griffith, J.; Mitchell, P.; Corey-Bloom, J.; Gluhm, S.; Goldstein, J.;
54 Levi, L.; Rosas, H. D.; Margolis, R.; Yoritomo, N.; Janicki, S.; Marder, K.; Clouse, R.; Singer,
55
56
57
58
59

1
2
3 C.; Moore, H.; Padron, N.; Kostyk, S.; Daley, A.; Segro, V.; Kumar, R.; Anderson, K.; Drazinic,
4 C.; Hennig, B.; Nance, M.; Molho, E.; Criswell, S.; LeDoux, M. S.; Guyot, S.; Iannaccone, A.;
5 Jennings, B.; Leavitt, B. R.; Feigin, A.; Evans, S.; Wray, S.; Casaceli, C.; Orme, C.; Gao, S.;
6 Oakes, D.; Watts, A.; Baker, K.; Labuschagne, I.; El-Dairi, M.; Fekrat, S.; Hersch, S.;
7 Moscovitch-Lopatin, M.; Angus, D.; Herd, C.; Stone, C.; Ritchie, C. W.; Tanzi, R.; Targum, S.,
8 Safety, tolerability, and efficacy of PBT2 in Huntington's disease: a phase 2, randomised,
9 double-blind, placebo-controlled trial. *Lancet Neurol.* **2015**, *14* (1), 39-47.

10
11 45. Liang, S. H.; Southon, A. G.; Fraser, B. H.; Krause-Heuer, A. M.; Zhang, B.; Shoup, T.
12 M.; Lewis, R.; Volitakis, I.; Han, Y.; Greguric, I.; Bush, A. I.; Vasdev, N., Novel Fluorinated 8-
13 Hydroxyquinoline Based Metal Ionophores for Exploring the Metal Hypothesis of Alzheimer's
14 Disease. *ACS Med. Chem. Lett.* **2015**, *6* (9), 1025-1029.

15
16 46. Nguyen, M.; Bijani, C.; Martins, N.; Meunier, B.; Robert, A., Transfer of Copper from an
17 Amyloid to a Natural Copper-Carrier Peptide with a Specific Mediating Ligand. *Chem. - Eur. J.*
18 **2015**, *21* (47), 17085-17090.

19
20 47. Nguyen, M.; Vendier, L.; Stigliani, J.-L.; Meunier, B.; Robert, A., Structures of the
21 Copper and Zinc Complexes of PBT2, a Chelating Agent Evaluated as Potential Drug for
22 Neurodegenerative Diseases. *European Journal of Inorganic Chemistry* **2017**, *2017* (3), 600-608.

23 48. <http://adisinsight.springer.com/drugs/800019374>.

24 49. Xiao, G.; Fan, Q.; Wang, X.; Zhou, B., Huntington disease arises from a combinatory
25 toxicity of polyglutamine and copper binding. *Proc. Natl. Acad. Sci. U. S. A.* **2013**, *110* (37),
26 14995-15000,S14995/1-S14995/5.
27
28
29
30
31
32
33
34
35
36
37
38
39
40
41
42
43
44
45
46
47
48
49
50
51
52
53
54
55
56
57
58
59
60